IOPscience iopscience.iop.org

Home Search Collections Journals About Contact us My IOPscience

Dynamical properties of an isolated step

This article has been downloaded from IOPscience. Please scroll down to see the full text article.

1996 J. Phys.: Condens. Matter 8 7589

(http://iopscience.iop.org/0953-8984/8/41/008)

View the table of contents for this issue, or go to the journal homepage for more

Download details:
IP Address: 171.66.16.207
The article was downloaded on 14/05/2010 at 04:17

Please note that terms and conditions apply.

J. Phys.: Condens. Matter **8** (1996) 7589–7603. Printed in the UK

Dynamical properties of an isolated step

A Virlouvet†, H Grimech†, A Khater†, Y Pennec‡ and K Maschke§

† Laboratoire de Physique des Matériaux, Unité de Recherche associée au CNRS 807, Université du Maine, F-72017 Le Mans Cédex, France

‡ Laboratoire de Structure et Propriétés de l'Etat Solide, Unité de Recherche associée au CNRS 234, Université de Lille I, F-59655 Villeneuve d'Ascq Cédex, France

§ Institut de Physique Appliquée, Ecole Polytechnique Fédérale, CH-1015 Lausanne, Switzerland

Received 4 January 1996

Abstract. The dynamics for a model system of an isolated infinite step in a surface are presented. The model is simple, treating the monatomic step as the interface between two coupled semi-infinite and single semi-infinite atomic layers. The breakdown of translational symmetry perpendicular to the step edge gives rise to several Rayleigh-like branches localized in the neighbourhood of the step. It is seen that a step may lift the polarization degeneracy of the ordered surface Rayleigh mode along the atomic rows parallel to and in the neighbourhood of the step edge. Typical dispersion curves for these modes along the step edge are given with their polarizations. The vibrational Green functions are calculated for the system, and the spectral densities are presented numerically for atomic sites that constitute a minimum representative set in the neighbourhood of the step. A hyperfine resonance structure is obtained that permits the analysis of the evolution of the dynamics from one half-space to the other.

1. Introduction

There has been increasing interest during the last decade in the theoretical and experimental study of the dynamics of disordered surfaces [1–9]. The presence of nanostructures such as random steps, kinks and other defects on crystal surfaces is important to their equilibrium topography as well as to a number of other surface properties.

This interest has also been motivated by the increasing need to refine the knowledge of substrate surfaces, and to acquire insight into their electronic and mechanical properties with a view to high-technology applications. For example, questions concerning the thermodynamic stability of vicinal surfaces [10–15] and the modes of their kinetic growth are becoming important and necessitate a better understanding of the role of disorder.

The study of dynamic phenomena at disordered surfaces by completely *ab-initio* techniques is still a difficult exercise, owing to the complexity of the phenomena, even though some empirical many-body potentials are available [16], and can lead to refinements in the numerical values attributed to force constants in the neighbourhood of surface defects, and to the relaxed positions of the atoms in vicinal surfaces.

Recently the problem of the dynamics of surface steps is being increasingly addressed. In one study [9], a local theoretical analysis of the dynamics of the step edge in a relaxed and reconstructed Ag(511) is given; in another [17], surface phonon dispersion curves of vicinal Cu(211) and Cu(511) have been measured, and the experimental data have been interpreted in terms of theoretical slab calculations in the framework of a single-force-constant model. In a more recent paper [18], the surface Rayleigh waves at a vicinal Ni(977) surface are

0953-8984/96/417589+15$19.50 © 1996 IOP Publishing Ltd

obtained in the long-wavelength limit using perturbation analysis and elasticity theory. The vicinal surfaces are treated in these studies as periodically stepped in the direction normal to the steps, and the calculations are carried out with corresponding boundary conditions, so that the model is effectively one dimensional in the direction normal to the average surface.

The case of an isolated step, to our knowledge, has not been treated yet. In this paper we do not study the full problem arising from the absence of translational symmetry in two directions due to a surface step. We present a precursor model system with the intention of studying the dynamics of an isolated surface step. Physically this system is representative of the case where the random distance between steps, e.g. in a vicinal surface, is greater than the coherence length of a surface phonon. Our model, a simple one based on two coupled semi-infinite atomic layers interfacing with a single semi-infinite atomic layer, as shown in figure 1, is one dimensional, but in this case the distinctive feature is a direction normal to the step edge rather than to the average surface.

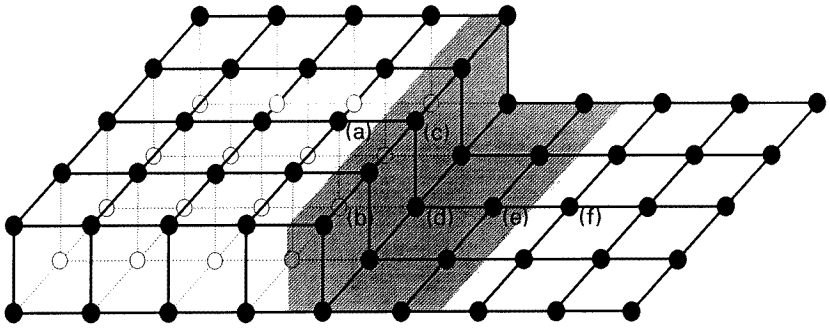

Figure 1. A schematic representation of an isolated infinite step, modelled as the interface between the two coupled and single atomic layers, in two separate half-spaces.

Low-dimensional models have long been of theoretical interest as systems which can yield useful information with well defined mathematical properties [19]. There is also renewed in these systems from another viewpoint, namely because of the need to understand the influence of local defects on the DC transport in mesoscopic quantum wires of finite widths. Although this is different with respect to the present considerations of lattice synamics, dealing instead with the electronic properties, nevertheless the underlying mathematical analysis is comparable [20].

Strictly the isolated infinite step in a surface is a system for which the translational symmetry is missing in two directions, perpendicular to the surface and the step edge. In our model the bulk is ignored and emphasis is put on the direction normal to the step edge. In section 2 we describe the theoretical model, and in section 3 the calculation of the phonon dispersion curves for the Rayleigh-like branches along the isolated step edge are given for a case study. In section 4 the real-space Green functions that describe the step edge dynamics are derived, and the spectral densities are obtained. The discussion and conclusions are presented in section 5.

2. The model of an isolated step edge and its evanescent dynamics

Our structural model is based on two coupled semi-infinite atomic layers interfacing with a single semi-infinite atomic layer, as shown in figure 1, with nearest- and next-nearest-

neighbour interactions, letting r denote their ratio in both semi-infinite parts of the system. Moreover, we allow for a modification of the strain field in the step region, the parameter λ denoting the ratio of these modified force constants to the constants of the system outside the step region. This region is defined as the grey area in figure 1.

A number of methods exist to study phonons and resonances in surfaces, [21–24]. The matching method which we employ in this paper [23] is one of them. It applies to the analysis of the dynamics of ordered surfaces by stipulating that localized surface modes should match the evanescent dynamics of the crystal bulk along the direction normal and away from the surface. This method has previously been extended to study low-dimensional models for phonon scattering by isolated defects [25]. The matching method allows us to deal with both aspects of localized modes and scattering of phonons at defects, within the same mathematical framework.

The equation of motion of an atom at site $\boldsymbol{l}$ is given as usual in the harmonic approximation [21] by

$$\omega^2 m(\boldsymbol{l})u_\alpha(\boldsymbol{l},\omega) = -\sum_{\boldsymbol{l}'\neq\boldsymbol{l}}\sum_{\beta} K(\boldsymbol{l},\boldsymbol{l}')\frac{r_\alpha r_\beta}{d^2}(u_\beta(\boldsymbol{l},\omega)-u_\beta(\boldsymbol{l}',\omega)) \tag{1}$$

for $(\alpha,\beta)\in\{x,y,z\}$, where $m\equiv m(\boldsymbol{l})$ is the atomic mass for sites $\boldsymbol{l}$, $u_\alpha(\boldsymbol{l},\omega)$ is the displacement field along the α direction, r_α is the corresponding cartesian component of the radius vector between $\boldsymbol{l}$ and $\boldsymbol{l}'$, d is the distance between $\boldsymbol{l}$ and $\boldsymbol{l}'$, and $K(\boldsymbol{l},\boldsymbol{l}')$ is the force constant between $\boldsymbol{l}$ and $\boldsymbol{l}'$. In this representation the x and y axes are taken normal and parallel, respectively, to the infinite step edge in figure 1. The z axis, not to be confused with the phase factors introduced later, is normal to the plane of the x and y axes.

The evanesence vibrational field in the two coupled and in the single atomic layers, away from the step region, is described by the phase factor doublets $(z(i),z(i)^{-1})$ and $(z(j)',z(j)'^{-1})$, respectively, going from one site to its nearest neighbours or vice versa along the direction normal to the step edge. Here $i(j)$ label the solutions in the infinite double (single) layers. The evanescence field, determined by the conditions $|z(i)|<1$ and $|z(j)'|<1$, is given by the evanscent solutions of the equations of motion.

Using equation (1), the atomic motion on a site (n_x,n_y) outside the step region, in the single atomic layer, can be expressed as

$$[\Omega^2 I - N(\varphi_y,z',r,\lambda)]|u'\rangle = |0\rangle \tag{2}$$

where the dimensionless frequency Ω is given by $\Omega^2 = m\omega^2/K(\boldsymbol{l},\boldsymbol{l}')$, l and l' are the sites of the nearest neighbours, and $\boldsymbol{\varphi}=a\boldsymbol{k}$, $\boldsymbol{k}$ being the one-dimensional reciprocal-lattice wavevector in the direction parallel to the step edge.

A similar set of equations is obtained for the two coupled atomic layers for the sites (n_x,n_y,n_z) and (n_x,n_y,n_{z-1}):

$$[\Omega^2 I - M(\varphi_y,z,r,\lambda)]|u\rangle = |0\rangle. \tag{3}$$

The detailed expressions for the dynamical matrices as functions of φ_y, r, λ and $z(z')$ are given in the appendix.

For these dynamical matrices in equations (2) and (3), a non-trivial solution requires that the determinants $\det[\Omega^2 I - N(\varphi_y,z',r,\lambda)]$ and $\det[\Omega^2 I - M(\varphi_y,z,r,\lambda)]$ vanish. This gives rise to two characteristic secular equations of degrees 12 in z and four in z', which may be expressed in the polynomial form

$$A_0 + A_1 z + A_2 z^2 + A_3 z^3 + A_4 z^4 + A_5 z^5 + A_6 z^6 + A_7 z^7 + A_8 z^8 + A_9 z^9 + A_{10} z^{10} + A_{11} z^{11} + A_{12} z^{12} = 0 \tag{4}$$

$$A'_0 + A'_1 z' + A'_2 z'^2 + A'_3 z'^3 + A'_4 z'^4 = 0 \tag{5}$$

where the coefficients A_n and A'_n are functions of Ω, φ_y, r and λ. We can show that both phase factors z and z^{-1}, as well as z' and z'^{-1}, verify symmetrically the polynomials, owing to the Hermitian nature of the bulk dynamics. To satisfy the evanescent conditions $|z| < 1$ and $|z'| < 1$, we select, however, only six physically acceptable solutions for z, and two for z', from the roots of equations (4) and (5). Together these solutions constitute in the space $\{\Omega, \varphi_y\}$ the set of evanescent modes $\{z(i), z'(j)\}$, $i \in \{1, 2, 3, 4, 5, 6\}$ and $j \in \{1, 2\}$. The evanescence field is then rigorously determined in the two semi-infinite parts of the model system.

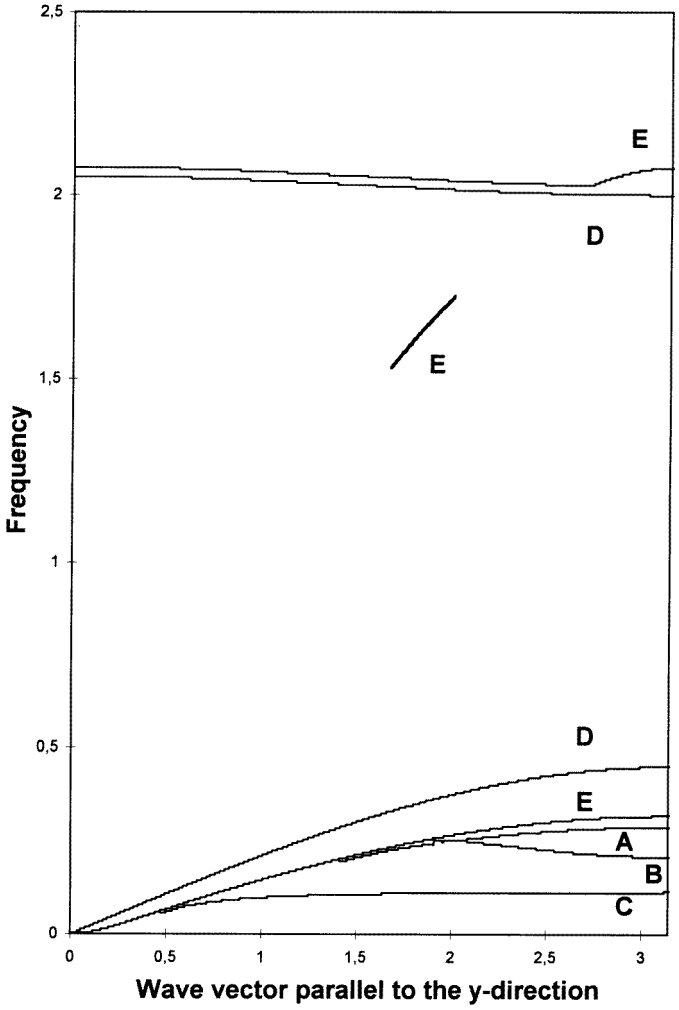

Figure 2. The localized Rayleigh step dispersion branches A, B and C as functions of the wavevector φ_y in the direction of high symmetry for the system along the y axis. D–D and E–E denote the bulk phonon band limits for the single layer, and for the coupled two atomic layers, respectively.

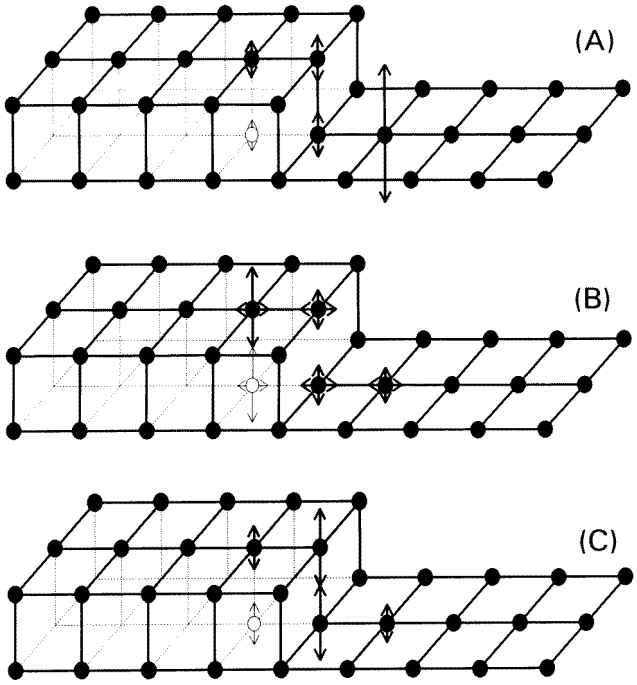

Figure 3. The arrows illustrate amplitudes or polarizations for the three localized Rayleigh step modes of figure 2, for a representative wavevector $\varphi_y = \frac{3}{4}\pi$.

3. Rayleigh modes on a model isolated step edge

The Cartesian components α of the displacements field for an atom outside the step domain, i.e. outside the grey area of figure 1, can be expressed [7, 23], as

$$u'_\alpha(n_x n_y) = \sum_{j=1}^{2} [z'(j)]^{n_x} R_j^+ p'(\alpha, j) \tag{6}$$

for an atomic site in the single atomic layer, and as

$$u_\alpha(n_x n_y n_z) = \sum_{i=1}^{6} [z(i)]^{-n_x} R_i^- p(\alpha, i) \tag{7}$$

for an atomic site in the two coupled atomic layers. R_j^+ and R_i^- are unit vectors spanning the space of the solutions corresponding to the set $\{z(i), z'(j)\}$. The coefficients $p(\alpha, i)$ and $p'(\alpha, j)$, identify the relative weighting factors associated with the different atomic displacements u_α and u'_α [7,21].

Denoting by $|R\rangle$ the basis vector in the constructed space, and by $|U\rangle$ that composed by a choice of a set of irreducible sites in the step region plus a minimum representative set of sites in the matching regions in the two semi-infinite domains of the system, the equations of motion for the step as an infinite defect can rewritten in terms of $|U\rangle$.

The necessary minimum set of sites defining the vector $|U\rangle$ is indicated in figure 1 by the letter (a), (b), (c), (d), (e) and (f). Taking (d) as the origin, their coordinates are as

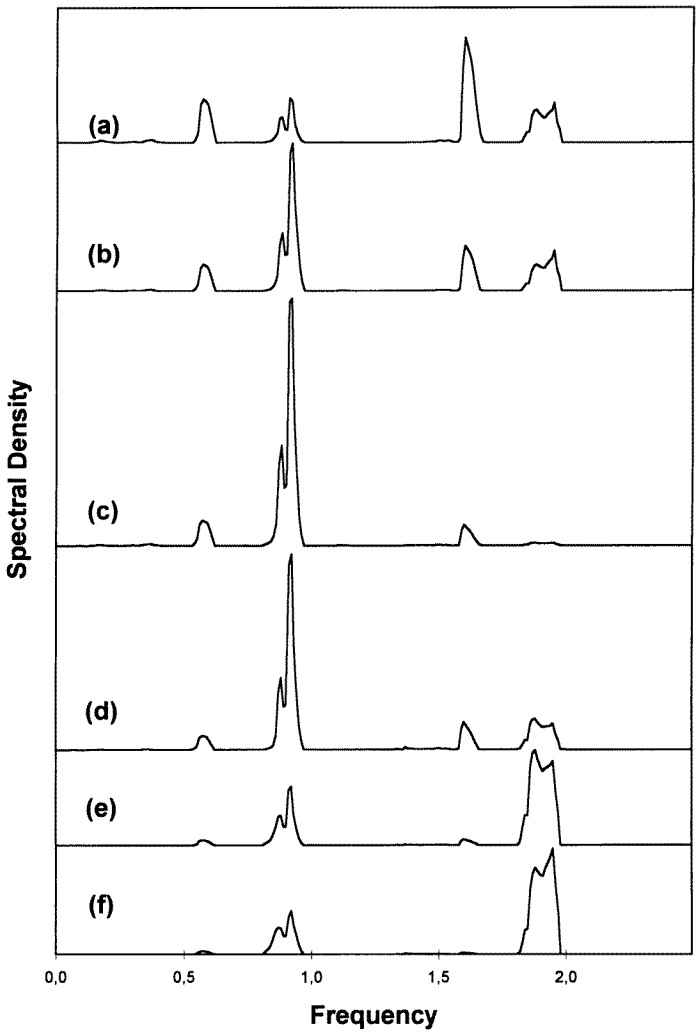

Figure 4. Phonon spectral densities in the direction of the x axis normal to the step edge, for all the atoms (a), (b), (c), (d), (e) and (f) in the minimum representative set of sites contained in the grey area of figure 1.

follows:

(a) $(-1, 0, +1)$ (b) $(-1, 0, 0)$ (c) $(0, 0, +1)$
(d) $(0, 0, 0)$ (e) $(+1, 0, 0)$ (f) $(+2, 0, 0)$

Using equations (3), (6) and (7), and the transformations connecting the two vectors $|R\rangle$ and $|U\rangle$ of interest, we obtain a square linear homogeneous system of equations

$$[\Omega^2 I - D(\varphi_y, r, \lambda, z(i), z'(j))]|U\rangle = |0\rangle \tag{8}$$

$i \in \{1, 2, 3, 4, 5, 6\}$, $j \in \{1, 2\}$. Note that all sites in the step region have three degrees of freedom for their atomic displacements, since we allow for next-nearest-neighbour interactions between the (n_x, n_y, n_z) sites on the step edge of the two coupled atomic layers

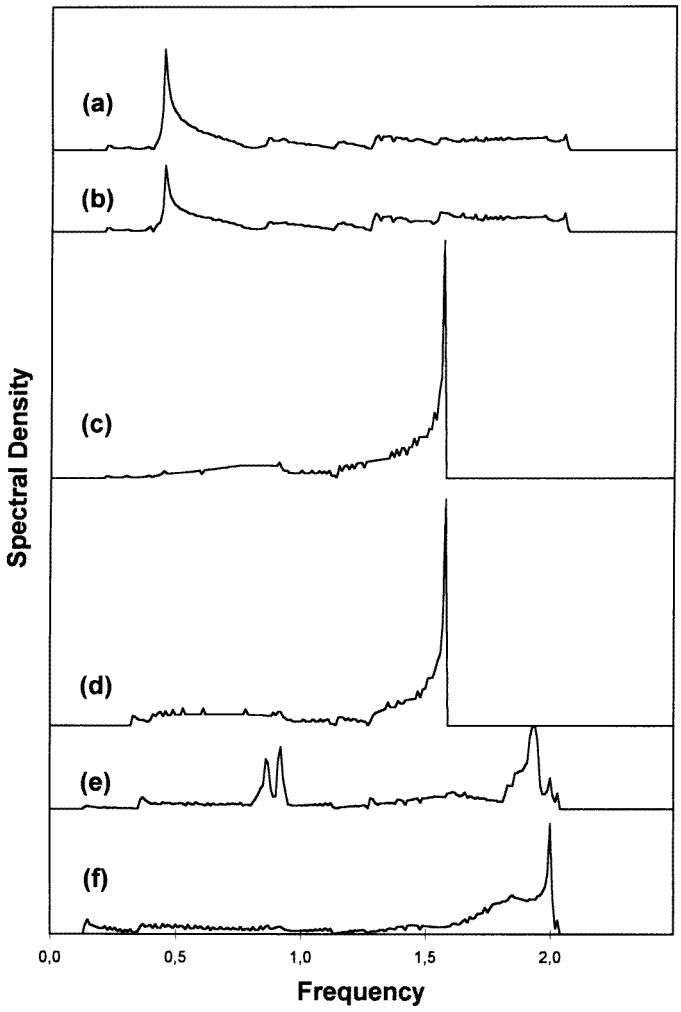

Figure 5. Phonon spectral density in the direction of the y axis parallel to the step edge for all the atoms (a), (b), (c), (d), (e) and (f) in the minimum representative set of sites contained in the grey area of figure 1.

with the sites (n_x, n_y) of the single atomic layer, in this region. The size of the vector $|U\rangle$ and the dimensions of equation (8) depend as a consequence directly on the necessary minimum set of atomic sites indicated above. A non-trivial solution yields the energies of the localized vibrational modes on the step, as a function of the system parameters.

To apply the model, numerical calculations may be obtained for a variety of values; we present here the case where $r = 0.05$, considering that next-nearest-neighbour interactions are much weaker than the nearest-neighbour interactions, and $\lambda = 0.6$ to illustrate the softening of the force constants in the step region [27]. These values are reasonable in a condensed-matter context.

Solving numerically the systems of equations (4) and (5) for itinerant solutions gives the phonon bulk band limits for the single atomic layer denoted by curves D, and those for the two coupled atomic layers denoted by curves E, respectively, in figure 2. We note

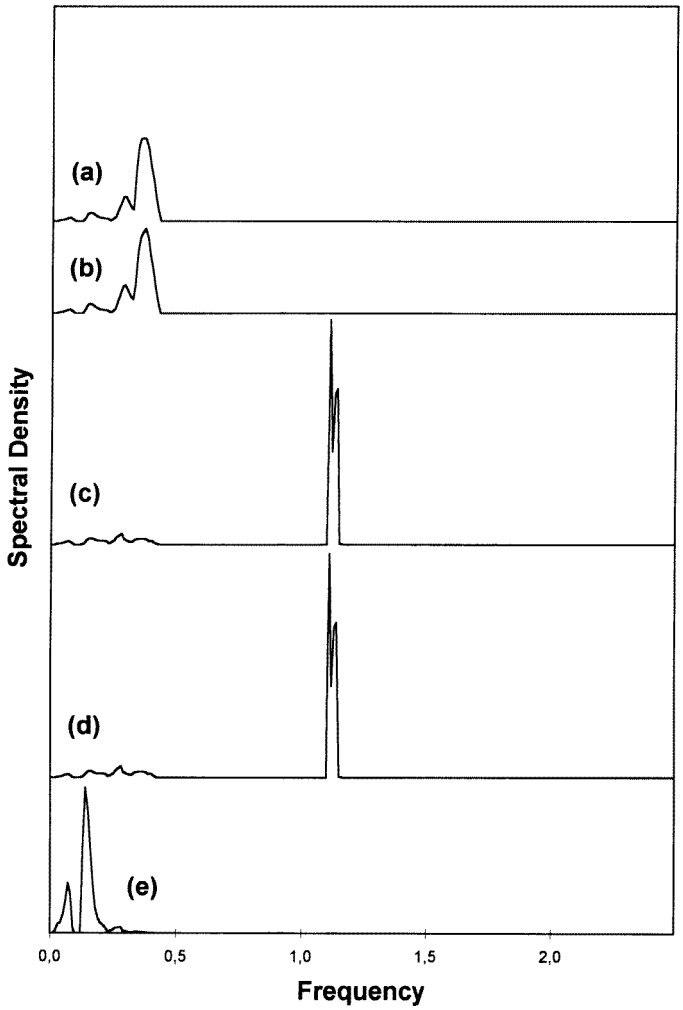

Figure 6. Phonon spectral density in the direction of the z axis normal to the system for all the atoms (a), (b), (c), (d) and (e) in the minimum representative set of sites contained in the grey area of figure 1.

the presence of a small and thin window in the bulk region which becomes larger when r increases. Note that the E–E band is similar to the projection of bulk phonon bands for an FCC crystal on a Miller low-index surface. This similitude may be made more striking still by adjusting appropriately the value of r. In figure 2, curves A, B and C represent the dispersion curves of the phonon modes localized on the isolated infinite step edge, illustrating how the breakdown of translational symmetry owing to the presence of a step may induce several new Rayleigh-like branches along a step edge in a surface. This is seemingly in qualitative agreement with the theoretical results of [18], although a detailed comparison shows that the natures of the modes are not the same in the two studies. In the cited work, Mele and Pykhtin label two of the branches as primary and secondary Rayleigh modes, the secondary being a back-folded excitation owing to the model periodicity of the Ni(977) vicinal surface. In our case there is no such folding; rather the A, B, and C Rayleigh

branches arise because the step lifts in real space the polarization degeneracy of an ordered surface Rayleigh mode along the atomic rows parallel to and in the neighbourhood of the step edge. Furthermore, our third mode B bears no resemblance to the third mode in [18] which is again due to Brillain zone folding. Note that the dispersion relations of modes A and B are not degenerate in the region $1.4 < \varphi_y < 2.1$.

The polarizations of mode B are such that the displacements on a couplet of sites, one above the other in the two layers, are symmetric. In contrast the polarizations of modes A and C are such that the displacements on an equivalent couplet of sites are antisymmetric. This is a confinement effect due to the finite extension of the two semi-infinite layers along the z axis.

Figure 3 shows by the use of arrows the relative amplitudes or polarizations on the sites, for an exemplifying wavevector φ_y fixed at $3\pi/4$. The first Rayleigh mode A is antisymmetric and characterized by amplitudes purely along the z axis, attaining a maximum on the site (e) off the step edge in the single-layer half-space. The second Rayleigh mode B is symmetric and characterized by amplitudes along the x and z axes, attaining a maximum on the sites couplet (a)–(b) off the step edge in the two-layer half-space. For the antisymmetric Rayleigh mode C the amplitudes are purely along the z axis; the maximum amplitude is for the sites (c) and (d) which are strictly on the step edge. Although not explicitly shown with additional arrows in figure 3, the amplitudes decrease exponentially as we move away from the step region in either sense along the direction normal to the step edge, in accord with the evanescence dynamics of the system.

4. The spectral densities of phonons on a model isolated step edge

The most direct manner to calculate the spectral densities is via the Green functions. It is possible for us to express the Green operator using the matching method [28], as

$$G(\varphi_y, \Omega^2 + \mathrm{i}\epsilon) = [(\Omega^2 + \mathrm{i}\epsilon)I - D(\varphi_y, r, \lambda, \{z\}, \{z'\})]^{-1}. \tag{9}$$

The phonon spectral density matrix, for a given wavevector parallel to the step edge, is then given by the following relation:

$$\rho^{(l,l')}_{(\alpha,\beta)}(\varphi_y, \Omega) = 2\Omega \sum_m P^l_{\alpha m} P^{l'*}_{\beta m} \delta(\Omega^2 - \Omega^2_m) \tag{10}$$

where $\boldsymbol{l}$ and $\boldsymbol{l}'$ represent two different atoms, α and β are two different Cartesian directions, and $P^l_{\alpha m}$ is the α component of the polarization vector on the atom at $\boldsymbol{l}$ for the mode of frequency Ω_m. The density of states can also be expressed as

$$N(\Omega) = \sum_{\varphi_y} \sum_{l\alpha} \rho^{(l,l)}_{(\alpha,\alpha)}(\varphi_y, \Omega) = -\frac{2\Omega}{\pi} \sum_{\varphi_y} \sum_{l\alpha} \lim_{\epsilon \to 0^+} \{\mathrm{Im}[G^{ll}_{\alpha\beta}(\varphi_y, \Omega^2 + \mathrm{i}\epsilon)]\} \tag{11}$$

summing over the trace of the matrix.

As shown in figures 4–6, we have calculated for each of the atomic sites (a), (b), (c), (d), (e) and (f) their phonon spectral densities along the Cartesian axes. For completeness we also plot in figures 7–9, the densities of states per site in the frequency range of interest.

5. Discussion and conclusions

Figure 4 gives the spectral densities along the x axis for the above atoms. Six resonance peaks are observed for all curves, in the range of Ω between 0.5 and 2. As can be seen in figure 2, this range which corresponds to the D–D frequency domain of the phonon

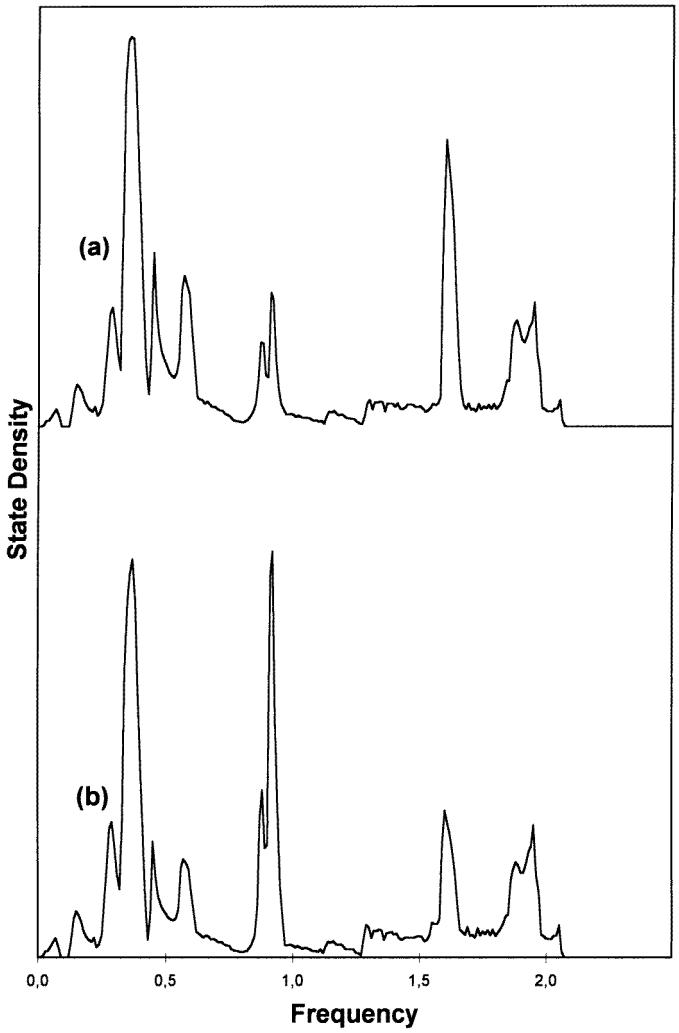

Figure 7. The density of states for the two sites (a) and (b) belonging to the two-atomic-layer half-space.

bulk band in the semi-infinite single atomic layer is contained in the E–E domain. This explains why all the sites, including those in the semi-infinite coupled atomic layers, have such resonances as well. The same phonons excite resonance simultaneously in both semi-infinite parts along the x axis normal to the step edge. There is no evidence for resonance outside the D–D domain which is to be expected. The site couplet (a)–(b), one atom above the other, has a highly analogous spectral structure; this is also true for the site couplet (c)–(d), as well as for (e) and (f) next to each other in the single layer. The corresponding spectra are not identical owing to the absence of symmetry for the overall system.

Figure 5 gives the spectral densities for these atoms along the y axis parallel to the step edge. In this direction of high symmetry for the system, there are several resonance peaks at frequencies other than those for the x-axis resonances. However, a similar couplet behaviour is observed for (a)–(b), and for (c)–(d) sites. The (e) atom has a double resonance

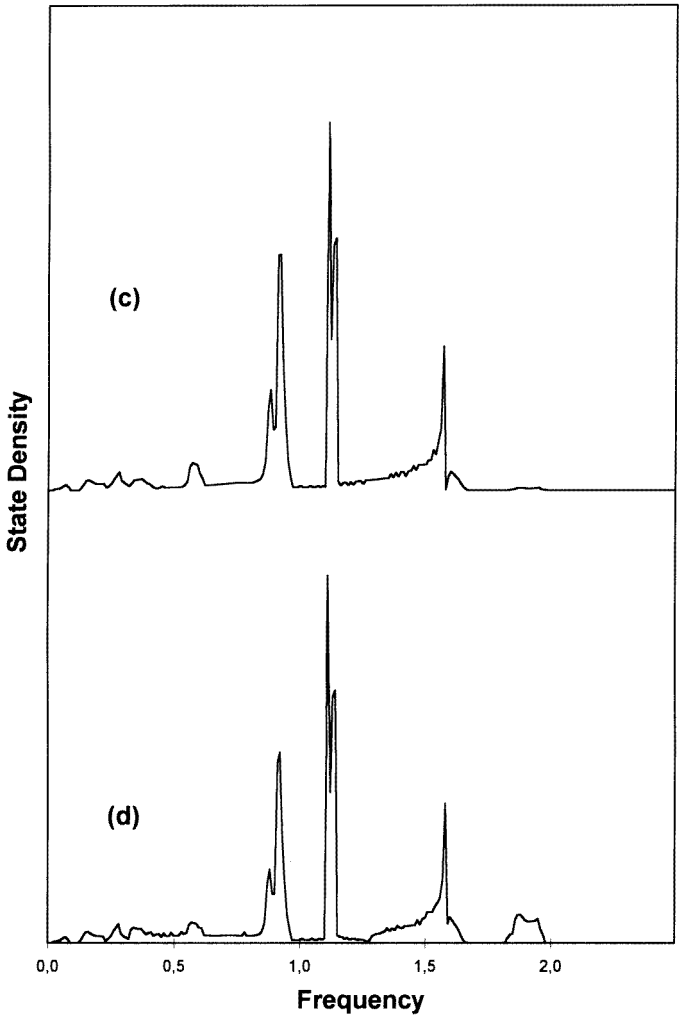

Figure 8. The density of states for the two sites (c) and (d) belonging to the two-atomic layer half-space, and for the (d) site interfacing with the single layer.

at $\Omega \simeq 0.85$ whereas the (f) atom does not along the z axis, although both have similar densities along the x axis. In the calculation the (e) site is allowed to have three degrees of liberty owing to its supposed next-nearest-neighbour interaction with the (c) site of the step edge. At $\Omega \simeq 0.85$ the (a), (b), (c) and (d) atoms on the double plane also have resonances, albeit small. It seems probable that (e) has a greater liberty along the y axis compared with these other sites, although the resonance at $\Omega \simeq 0.85$ follows from an interaction along the z axis.

The spectral densities along the z axis are shown in figure 6. The sites of the couplet (a)–(b) have identical spectral densities, with four overlapping peaks. The two high-frequency peaks can be attributed to bulk resonances. The two low-frequency peaks, in contrast, are due to the excitation by the localized Rayleigh like modes along the step edge, as can be seen with reference to figures 2 and 3. We observe a similar behaviour for the site couplet

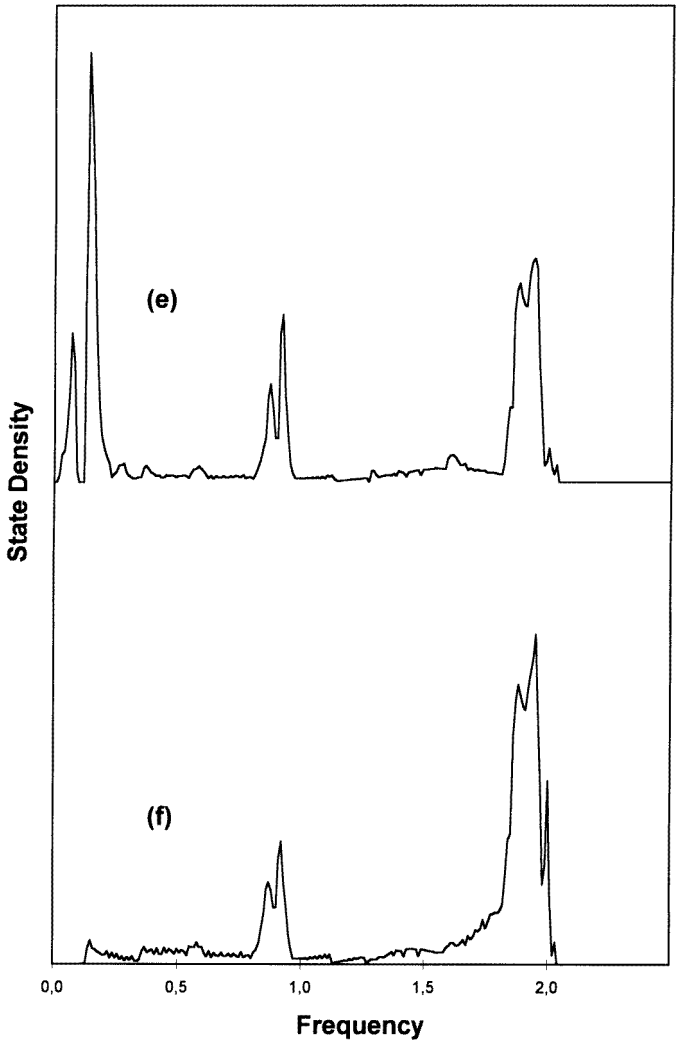

Figure 9. The density of states for the two sites (e) and (f) belonging to the single-atomic-layer half-space.

(c)–(d); in this case, however, it is difficult to say whether the exciting modes come from the bulk of the single or double atomic layers. Finally the resonances on site (e) are again determined by its extra degree of freedom along the z axis; it is hence evident that this resonance is associated with the excitation of the localized Rayleigh-like modes travelling along the step edge, given the ranges of their frequencies and polarizations. The site (f) has only two degrees of freedom along the x and y axes, has no renonances along the z axis and is not presented in figure 6.

For completeness we plot in figures 7–9, the densities of states per atomic site, in the frequency interval of interest, for the sites considered. for the couplets (a)–(b) and (c)–(d), these densities are quite similar, as may be expected. They are not identical owing to the absence of symmetry along the z axis for the overall system. The densities of state for

the (e) and (f) sites are similar over the high-frequency range in the phonon bulk band of the single atomic layer, but quite different in the range of low frequencies typical of the step localized modes A, B and C. At low frequencies the (e) site registers a remarkable contribution from these modes.

It is interesting to compare our results with previous ones, notably with those in reference [27], which are sufficiently systematic to be useful for our purpose. However, one should be careful in this exercise for a number of reasons. First of all the system studied by Tian *et al* is an FCC slab which presents an ordered $(1, 1, n)$ stepped surface whereas ours is a simple cubic thin slab with an isolated step. To make any sense of this we compare our results with those for a high index $(1, 1, n)$ namely the $(1, 1, 13)$ on which the ordered steps are nevertheless far apart, and for which these authors provide systematic results. Ideally we should have results in their work for an infinite n, for a realistic comparison with our isolated step. We compare the spectral densities for sites which are most comparable in the two works, namely sites c here with their S, e here with their T, and d here with their C.

Concerning the (c, S) sites our results for the c site show clearly identifiable peaks compared to those for the S site. Nevertheless the dominant peak in the two spectra has a similar behaviour, with peak positions following the sequence $\Omega(x) < \Omega(y) < \Omega(z)$. Considering the (e, T) sites, the e site presents the same doublet as the T site in [27], with approximately the same doubling of the frequency for the x and y polarizations. However, the spectral density for z shows a difference between the two model treatments. The spectral density of e along z in our work, as pointed out earlier, is closely associated to the localized Rayleigh like modes along the step edge. Since the model surface $(1, 1, 13)$ is an ordered arrangement of steps these modes may be absent or submerged for the T site, in any case we find no discussion concerning these modes in the work of Tian *et al*. As regards the (d, C) sites, four modes are apparent in both treatments for x, although it is difficult to make a realistic comparison. For the y polarization the same continuum appears in both model treatments leading up to a high frequency sharp peak for both d and C sites. For z this peak persists in our results but is absent in [27]. The qualitative similarities are interesting to point out despite the important structural and model differences: thin versus thick slab models, an isolated step versus an ordered $(1, 1, 13)$ stepped surface, cubic versus FCC structures, force constants versus embedded atom potential.

In our work the fine structure of the spectra and its origins are now clearly identifiable, which situation yields a new insight for this problem. In addition the existence and nature of the localized Rayleigh like modes associated to an isolated surface step are derived, and further the importance of the contributions of these modes to the spectral densities are highlighted for the first time, despite the apparent model simplicity.

The dynamics for a simple model system of an isolated infinite step in a surface are presented. It is seen that the breakdown of translational symmetry normal to the step edge may give rise to several vibrational modes that are Rayleigh-like branches localized in the neighbourhood of the step. Typical dispersion curves for these along the step edge ar given with their polarizations, and it is concluded that the step lifts the real-space polarization degeneracy of an ordered surface Rayleigh mode along the atomic rows parallel to and in the neighbourhood of the step edge. The vibrational real-space Green functions are calculated, and typical spectral densities are presented numerically for atomic sites in the neighbourhood of the step. A hyperfine resonance structure is thus obtained that permits the analysis of the evolution of the dynamics from one half-space to the other.

Appendix

The equations of atomic motion on the site (n_x, n_y) in the bulk of the monatomic layer can be expressed by

$$[\Omega^2 I - N(\varphi_y, z, r)]|u'\rangle = |0\rangle \tag{A1}$$

with

$$|u'\rangle = \begin{bmatrix} U'_x & (n_x, n_y) \\ U'_y & (n_x, n_y) \end{bmatrix} \tag{A2}$$

and

$$[N] = \begin{bmatrix} N(1) & N(3) \\ N(3) & N(2) \end{bmatrix} \tag{A3}$$

where

$$\begin{aligned} N(1) &= \Omega^2 + (z' + z'^{-1})(1 + r\cos\varphi_y) - 2r - 2 \\ N(2) &= \Omega^2 + \cos\varphi_y\,(2 + r(z' + x'^{-1})) - 2r - 2 \\ N(3) &= \mathrm{i}r\sin\varphi_y(z' - z'^{-1}). \end{aligned} \tag{A4}$$

The equations of atomic motion on the sites (n_x, n_y, n_z) in the bulk of the two coupled atomic layers can also be expressed in a resumed form as

$$[\Omega^2 I - M(\varphi_y, z, r)]|u\rangle = |0\rangle \tag{A5}$$

with

$$|u\rangle = \begin{bmatrix} U_x & (n_x, n_y, n_z) \\ U_y & (n_x, n_y, n_z) \\ U_z & (n_x, n_y, n_z) \\ U_x & (n_x, n_y, n_{z-1}) \\ U_y & (n_x, n_y, n_{z-1}) \\ U_z & (n_x, n_y, n_{z-1}) \end{bmatrix} \tag{A6}$$

and

$$[M] = \begin{bmatrix} M(1) & M(4) & 0 & M(5) & 0 & M(6) \\ M(4) & M(2) & 0 & 0 & M(7) & M(8) \\ 0 & 0 & M(3) & M(6) & M(8) & M(9) \\ M(5) & 0 & -M(6) & M(1) & M(4) & 0 \\ 0 & M(7) & -M(8) & M(4) & M(2) & 0 \\ -M(6) & -M(8) & M(9) & 0 & 0 & M(3) \end{bmatrix} \tag{A7}$$

where

$$\begin{aligned} M(1) &= -(z + z^{-1})(1 + r\cos\varphi_y) + 2 + 3r \\ M(2) &= -\cos\varphi_y\,(2 + r(z + z^{-1})) + 2 + 3r \\ M(3) &= 2r + 1 \\ M(4) &= \mathrm{i}(z - z^{-1})r\sin\varphi_y \\ M(5) &= \frac{r}{2}(z + z^{-1}) \\ M(6) &= -\frac{r}{2}(z - z^{-1}) \\ M(7) &= r\cos\varphi_y \\ M(8) &= -\mathrm{i}r\sin\varphi_y \\ M(9) &= \frac{r}{2}(z + z^{-1} + 2\cos\varphi_y) + 1 \end{aligned} \tag{A8}$$

References

[1] Armand G and Masri P 1983 *Surf. Sci.* **130** 89
[2] Black J E and Bopp P 1984 *Surf. Sci.* **140** 275
[3] Knipp P 1991 *Phys. Rev.* B **43** 6908
Knipp P and Hall B M 1989 *Surf. Sci.* **224** 983
[4] Lock A, Toennies J P and Witte G 1990 *J. Electron. Spectrosc. and Related Phenon.* **54–5** 309
[5] Bartoloni A, Ercolessi F and Tosatti E 1989 *Phys. Rev. Lett.* **63** 872
[6] Pennec Y, Rafil O and Khater A 1993 *J. Electron. Spectrosc. and Related Phenon.* **64–5** 777
[7] Pennec Y and Khater A 1995 *Surf. Sci. Lett.* **348** 82
[8] Watson G M, Gibbs D and Zehner D M 1994 *Phys. Rev. Lett.* **71** 3166
[9] Kara A, Jayanthi C S, Wu S Y and Ercolessi F 1993 *Phys. Rev. Lett.* **72** 2223
[10] Williams E D 1994 *Surf. Sci.* **299–300** 502
[11] Ebert P, Lagally M G and Urban K 1993 *Phys. Rev. Lett.* **71** 1437
[12] Kunkel R, Poelsema B, Verheij L K and Comsa G 1990 *Phys. Lett.* **65** 733
Michley T, Besocke K H and Comsa G 1990 *Surf. Sci.* **230** L135
[13] Barbier L, Salanon B and Sproesser J 1995 *J. Vac. Sci. Technol.* A **13** 117
[14] Ernst H-J, Fabre F and Lapujoulade J 1994 *J. Vac. Sci. Technol.* A **12** 1809
[15] Tian Z T and Rahman T 1993 *Phys. Rev.* B **47** 9751
[16] Daw M S and Baskes M I 1984 *Phys. Rev.* B **29** 6443
Jacobsen K W, Norskov J K and Puska M J 1987 *Phys. Rev.* B **35** 7423
[17] Witte G, Braun J, Lock A and Toennies J P 1995 *Phys. Rev.* B **52** 2165
[18] Mele E J and Pykhtin M V 1995 *Phys. Rev. Lett.* **75** 3878
[19] Lieb E H and Mattis D C (ed) 1966 *Mathematical Physics in One Dimension* (New York: Academic)
[20] Bertod C, Gagel F and Maschke K 1994 *Phys. Rev.* B **50** 18 299
[21] Maradudin A A, Wallis R F and Dobrzynski L 1980 *Handbook of Surfaces and Interfaces* vol 3 (New York: Garland)
[22] Feuchtwang T E 1967 *Phys. Rev.* **155** 715, 731
[23] Szeftel J and Khater A 1987 *J. Phys. C: Solid State Phys.* **20** 4725
[24] Allen R E, Alldredge G P and de Wette F W 1971 *Phys. Rev.* B **4** 1648
[25] Khater A, Auby N and Wallis R F 1989 *Surf. Sci.* **217** 563
Khater A, Auby N and Kechrakos D 1994 *J. Phys.: Condens. Matter* **4** 3743
[26] Kress W and de Wette F W (eds) 1991 *Surface Phonons* (Heidelberg: Springer)
[27] Tian Z-J and Black J E 1994 *Surf. Sci.* **303** 395
[28] Grimech H and Khater A 1995 *Surf. Sci.* **323** 198